analytical chemistry

pubs.acs.org/ac Article

Biocapture-Directed Chemical Labeling for Discerning Stressed States of Organelles

Lei Gao, Yilong Shi, Enkang Zhang, Jinxuan You, Jiahuai Han, Xinhui Su,* and Shoufa Han*

Cite This: *Anal. Chem.* 2022, 94, 9903−9910 Read Online

ACCESS | Metrics & More | Article Recommendations | Supporting Information

ABSTRACT: Lysosomal rupture engaged in diverse diseases remains poorly discerned from lysosomal membrane permeabilization (LMP). We herein reported biocapture-directed chemical labeling (BCCL) for the discern of lysosomal rupture by tracking the release of optically labeled cathepsins from damaged lysosomes into the cytosol. BCCL entails covalent anchoring of an azide-tagged suicide substrate (Epo-LeuTyr^{Az}) to the enzyme active site and bioorthogonal ligation of the introduced azide with ^{DBCO}RC, a ratiometric sensor featuring an acidity-reporting red emissive X-rhodamine-lactam (ROX), blue emissive coumarin (CM) inert to pH, and DBCO reactive to azide. Aided with fluorescein isocyanate-labeled sialic acid (FITC-Sia), a probe remained in pH-elevated lysosomes but dissipated from LMP$^+$ lysosomes, BCCL enables optical discern of four states of lysosomes: ruptured lysosomes (blue in cytosol), LMP$^+$ lysosomes (blue in lysosomes), pH-elevated lysosomes (blue and green in lysosomes), and physiological lysosomes (blue, green and red in lysosomes). This approach could find applicability to study lysosome rupture over LMP in diseases and to evaluate lysosome rupture-inducing drugs.

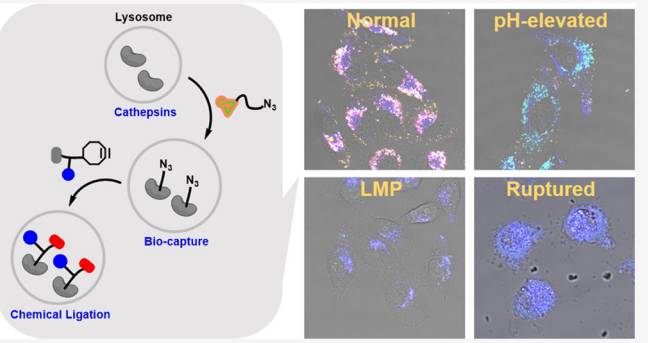

Lysosomes are membrane-bound organelles that sequester diverse hydrolytic enzymes in acidic lumen to degrade materials delivered from the inside and outside of cells, a process critical for cellular homeostasis, metabolism, and immunity.[1,2] Disruption of this hierarchy has been linked to myriad pathological disorders.[3−5] For instance, rupture of lysosomes releases resident cathepsins into cytosol, whereby cathepsins degrade key cytosolic proteins to execute cell death.[6−10] Given the role of lysosomal rupture to execute cell death, lysosome rupture inducers are actively explored for cancer treatment.[11] As such, optical techniques capable of discerning lysosomal rupture are of significance both to study lysosome rupture-engaged diseases and to evaluate inducers of lysosome rupture.

Over time, imaging of lysosomal rupture has been attempted with the use of acridine orange,[12,13] galectin,[14] or fluorescein isothiocyanante-labeled-dextran (FITC-dextran).[4] Acridine orange is an acidotropic dye that accumulates in lysosomes driven by lysosomal acidity. Therefore, acridine orange readily dissipates from pH-elevated lysosomes with intact lysosomal membrane or LMP$^+$ lysosomes due to loss of lysosomal acidity and permeabilized membrane, respectively. FITC-dextran is a polymeric microbead that is delivered into lysosomes by endocytosis. Although maintained in pH-elevated lysosomes, FITC-dextran could dissipate from lysosomes as a consequence of lysosome rupture as well as LMP. Similarly, recruits of galectin-3 occurred in both ruptured lysosomes and LMP$^+$ lysosomes.[15] Given the aforementioned limitations of current methods, it is imperative to discern lysosome rupture from LMP and pH-elevated lysosomes. Lysosomal rupture allows the release of hydrolases with a molecular weight greater than 4.4 kDa to the cytosol (such as cysteine cathepsins),[16] a feature absent in pH-elevated lysosomes and LMP. On the basis of these observations, we envisioned that cathepsin with dual-colored tags to pinpoint its subcellular location and surrounding pH could be employed to identify lysosome rupture (cathepsin in cytosol) from pH-elevated lysosomes and LMP (cathepsin in lysosomes).

On the basis of activity-based probes of cysteine cathepsins,[17−23] we opt a stepwise approach referred to as biocapture-directed chemical ligation (BCCL) for effective cathepsin labeling to define lysosome rupture (Figure 1). First, Epo-LeuTyr^{Az}, a leucine-tyrosine dipeptide with N-terminal epoxide and C-terminal azide, was designed to form covalent substrate−enzyme adduct via reaction of active site cysteine with epoxide moiety. Next, the substrate−enzyme adduct was

Received: April 29, 2022
Accepted: June 8, 2022
Published: June 27, 2022

https://doi.org/10.1021/acs.analchem.2c01892
Anal. Chem. 2022, 94, 9903−9910

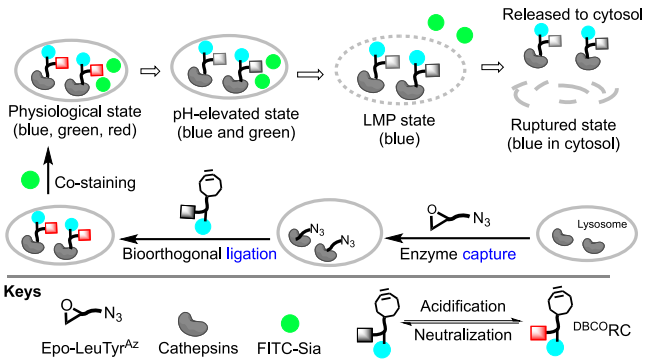

Figure 1. Schematic for discern of stressed lysosomes with BCCL. Cell culturing with Epo-LeuTyr^{Az} leads to covalent incorporation of azide into the active site of cathepsins. Further ligation of the azide with ^{DBCO}RC enables labeling of cathepsins with a dual-colored pH sensor. Integrating FITC-Sia prone to dissipation from LMP$^+$ or ruptured lysosomes, BCCL allows optical discern of four states of lysosomes: ruptured lysosomes (blue in cytosol) over LMP$^+$ lysosomes, pH-elevated and normal lysosomes.

further elaborated via stain-promoted azide−alkyne cycloaddition (SPAAC) between the introduced azide and ^{DBCO}RC, a ratiometric pH sensor composed of a DBCO moiety reactive to azide, an entity of X-rhodamine-lactam (ROX) with an acidity-reporting red emissive and an entity of coumarin (CM) with always-on blue fluorescence. Cells subjected to BCCL were further stained with FITC-Sia that exhibited green fluorescence in normal or pH-elevated lysosomes but null fluorescence in LMP$^+$ or ruptured lysosomes due to probe dissipation. This combination allows optical discern of four states of lysosomes: ruptured lysosomes (blue in cytosol), LMP$^+$ lysosomes (blue in lysosomes), pH-elevated lysosomes (blue and green in lysosomes), and physiological lysosomes (blue, green and red in lysosomes) (Figure 1).

EXPERIMENTAL PROCEDURES

Materials and Methods. Bafilomycin A1 (Baf-A1), TNF, Smac, Z-VAD, and FTIC-dextran (M_w = 40 kDa) were purchased from Selleck. All other chemicals were purchased from Sigma unless specified. HeLa cells were obtained from American Type Culture Collection, LAMP2-GFP$^+$ HeLa, LAMP2-RFP$^+$ HeLa, LAMP2-GFP-RIP$_3^+$ HeLa, and RIP$_3^+$ HeLa were prepared according to a reported procedure.[15,24,25] The cells were cultured in Dulbecco's modified Eagle's medium (DMEM; GIBCO, C11995500CP) supplemented with 10% fetal bovine serum (Thermo, A3160901), 2 mM L-glutamine (Millipore, TMS-002-C), 100 IU penicillin (Gibco, 15,140,122), and 100 mg/mL streptomycin (Sangon, A610494-0050) at 37 °C in a humidified incubator under 5% CO_2.

The fluorescence spectra were collected with SpectraMax M5. Confocal microscopic images were obtained on Leica SP8 using the following filters: λ_{ex} = 405 nm and λ_{em} = 415−485 nm for coumarin, λ_{ex} = 488 nm and λ_{em} = 498−550 nm for FITC and GFP, λ_{ex} = 552 nm, and λ_{em} = 562−630 nm for rhodamine, and red fluorescent protein (RFP). Images of merged fluorescence were processed with LAS X and Photoshop CS6.

In Vitro SPAAC of Epo-LeuTyr^{Az} with ^{DBCO}CM. To a flask containing CH_3OH (1 mL) were added Epo-LeuTyr^{Az} (6.86 mg, 0.01 mmol) and ^{DBCO}CM (12.4 mg, 0.02 mmol). The reaction solution was stirred for 30 min at room temperature. The mixture was analyzed by MALDI-TOF MS. MALDI-TOF MS calculated for $C_{67}H_{83}N_{15}O_{13}$ (M + Na^+) m/z 1329.49, found 1329.600, and $C_{103}H_{120}N_{20}O_{18}$ (M + Na^+) m/z 1949.22, found 1949.044.

Cell Staining with Epo-LeuTyr-CM. HeLa cells were cultured with Epo-LeuTyr-CM (10 μM) for 4 h, The cells were washed with DMEM three times at 37 °C, maintained in fresh DMEM, and then analyzed by confocal fluorescence microscopy.

Imaging of pH-Elevated Lysosomes and LMP with Epo-LeuTyr^{Az}/^{DBCO}CM. *Imaging of pH-Elevated Lysosomes.* LAMP2-GFP$^+$ HeLa cells were cultured with Epo-LeuTyr^{Az} (0, 20 μM) for 12 h. These cells were washed with DMEM and then incubated with ^{DBCO}CM (10 μM) for 2 h. These cells were again washed with DMEM and then maintained in DMEM containing Baf-A1 (0, 100 nM) for 6 h. The cells were washed with DMEM and then imaged with confocal microscopy.

LMP Imaging. AMP2-GFP$^+$ HeLa cells were cultured with Epo-LeuTyr^{Az} (0, 20 μM) for 12 h, washed with DMEM, and then incubated with ^{DBCO}CM (10 μM) for 2 h. These cells were then maintained in DMEM containing H_2O_2 (0, 0.5 mM) for 1 h. The cells were rinsed with DMEM and then imaged with confocal microscopy.

Imaging of Methanol-Induced LMP with Epo-LeuTyr^{Az}/^{DBCO}CM. LAMP2-GFP$^+$ HeLa cells were cultured with Epo-LeuTyr^{Az} (0, 20 μM) for 12 h, rinsed and washed with DMEM, and then incubated with ^{DBCO}CM (10 μM) for 2 h. These cells were further treated with MeOH (−20 °C) for 20 min before being maintained in PBS and then imaged with confocal microscopy.

Dose-Dependent and Time-Dependent Cell Staining with Epo-LeuTyrAz/^{DBCO}CM. LAMP2-GFP$^+$ HeLa cells were incubated with Epo-LeuTyr^{Az} (0, 10, 20, 50, and 100 μM) for 12 h, washed with DMEM, and then incubated with ^{DBCO}CM (10 μM) for 2 h. The cells were rinsed with DMEM and then imaged with confocal microscopy. These cells were further treated with MeOH (−20 °C) for 20 min before being maintained in PBS and imaged with confocal microscopy.

LAMP2-GFP$^+$ HeLa cells were cultured with Epo-LeuTyr^{Az} (20 μM) for 2, 4, 8, or 12 h. These cells were washed with DMEM and then incubated with ^{DBCO}CM (10 μM) for 2 h. The cells were washed with DMEM and then imaged with confocal microscopy. These cells were further treated with MeOH (−20 °C) for 20 min before being maintained in PBS and imaged with confocal microscopy.

Effects of Epo-LeuTyr^{Az} on LLOMe-Mediated LMP. LAMP2-RFP$^+$ HeLa cells were cultured with Epo-LeuTyr^{Az} (0, 20 μM) and FITC-dextran (0.1 mg/mL) for 12 h. These cells were washed with DMEM and then maintained in DMEM containing LLOMe (0, 3 mM) for 6 h. The cells were washed with DMEM and then imaged with confocal microscopy.

Imaging of Lysosome Rupture with Epo-LeuTyr^{Az}/^{DBCO}CM. LAMP2-GFP-RIP$_3^+$ HeLa cells were cultured with Epo-LeuTyr^{Az} (20 μM) for 12 h, then washed with DMEM and incubated with ^{DBCO}CM (10 μM) for 2 h. These cells were cultured for 5 h with TNF (60 ng/mL)/Smac (200 nM), or TNF (60 ng/mL)/Smac (200 nM)/Z-VAD (40 μM). The cells were washed with DMEM and imaged with confocal microscopy.

pH Titration of ^{DBCO}RC and FITC-Sia. ^{DBCO}RC or FITC-Sia were added to sodium phosphate buffer (10 mM) containing 30% CH_3CN (pH: 4.0, 4.5, 5.0, 5.5, 6.0, 6.5, 7.0,

https://doi.org/10.1021/acs.analchem.2c01892
Anal. Chem. 2022, 94, 9903−9910

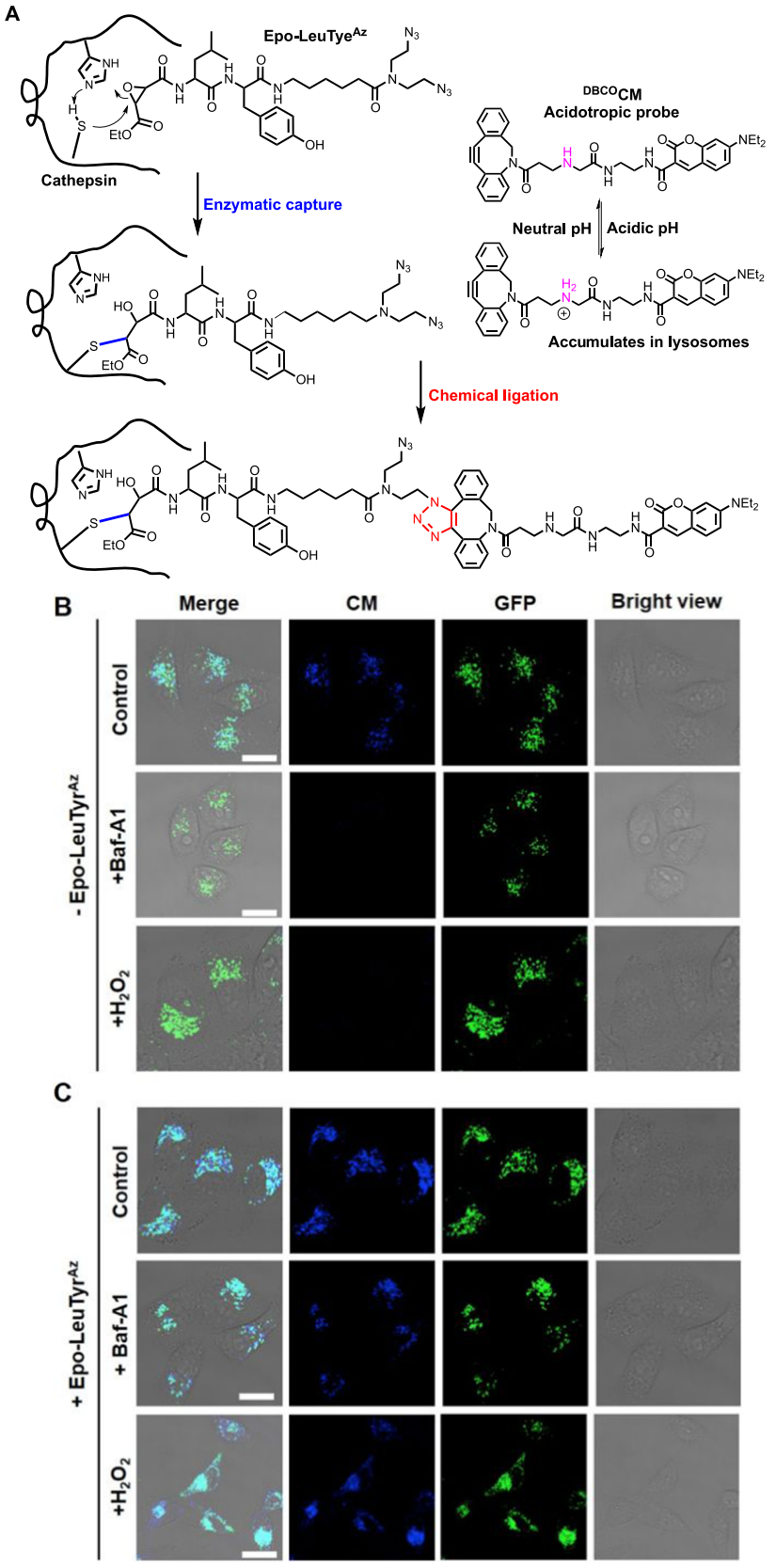

Figure 2. BCCL for cathepsin labeling in lysosomes. (A) BCCL with Epo-LeuTyr^{Az} and ^{DBCO}CM. (B) Incapability of ^{DBCO}CM to tag cathepsins and loss of ^{DBCO}CM from pH-elevated or LMP^{+} lysosomes. LAMP2-GFP^{+} HeLa cells were stained with ^{DBCO}CM (10 μM) for 2 h, and then treated with no addition (6 h), Baf-A1 (100 nM, 6 h), or H_2O_2 (0.5 mM, 1 h) prior to confocal analysis. (C) BCCL-conferred retention of ^{DBCO}CM in pH-elevated or LMP^{+} lysosomes. LAMP2-GFP^{+} HeLa cells were stained with Epo-LeuTyr^{Az} (20 μM, 12 h) and then with ^{DBCO}CM (10 μM, 2 h). The cells were further treated with Baf-A1 (100 nM, 6 h), no addition (6 h), or H_2O_2 (0.5 mM, 1 h) and then imaged by confocal microscopy. Scale bars: 10 μm.

https://doi.org/10.1021/acs.analchem.2c01892
Anal. Chem. 2022, 94, 9903−9910

7.5, 8.0, 8.5, 9.0) to a final concentration of 10 μM, respectively. The solution was analyzed for coumarin emission using λ_{ex} = 435 nm, fluorescence emission using λ_{ex} = 500 nm, and rhodamine emission using λ_{ex} = 590 nm.

Imaging of pH-Elevated Lysosomes and LMP with Epo-LeuTyr^{Az}/^{DBCO}RC. *Imaging of pH-Elevated Lysosomes.* LAMP2-GFP$^+$ HeLa cells were cultured with Epo-LeuTyr^{Az} (0, 20 μM) for 12 h. These cells were washed with DMEM and then cultured with ^{DBCO}RC (10 μM) for 2 h. These cells were washed with DMEM and then maintained in DMEM containing Baf-A1 (100 nM) for 6 h. The cells were washed with DMEM and then imaged with confocal microscopy.

LMP Imaging. LAMP2-GFP$^+$ HeLa cells were cultured with Epo-LeuTyr^{Az} (0, 20 μM) for 12 h. These cells were washed with DMEM and then incubated with ^{DBCO}RC (10 μM) for 2 h. These cells were cultured with DMEM containing H_2O_2 (0.5 mM) for 1 h. The cells were washed with DMEM and imaged with confocal microscopy.

Imaging of pH-Elevated Lysosomes and LMP with FITC-Sia Compared to FITC-Dextran. LAMP2-GFP$^+$ HeLa cells were cultured with FITC-Sia (10 μM) for 12 h or with FITC-dextran (0.1 mg/mL) for 12 h. These cells were washed with DMEM and then maintained in DMEM containing Baf-A1 (0, 100 nM) for 6 h or H_2O_2 (0.5 mM) for 1 h. The cells were washed with DMEM and imaged with confocal microscopy.

Imaging of pH-Elevated Lysosomes and LMP with Epo-LeuTyr^{Az}/^{DBCO}RC and FITC-Sia. HeLa cells were cultured with Epo-LeuTyr^{Az} (20 μM) and FITC-Sia (10 μM) for 12 h. These cells were washed with DMEM and then incubated with ^{DBCO}RC (10 μM) for 2 h. These cells were washed with DMEM and then maintained in DMEM containing Baf-A1 (0, 100 nM) for 6 h or H_2O_2 (0.5 mM) for 1 h. The cells were washed with DMEM and imaged with confocal microscopy.

Cytotoxicity of Probes. HeLa cells were cultured for 24 h with Epo-LeuTyr^{Az} (0, 1, 10, 25, 50 μM), ^{DBCO}CM (0, 1, 10, 25, 50 μM), ^{DBCO}RC (0, 1, 10, 25, 50 μM), or FITC-Sia (0, 1, 10, 25, 50 μM). Cell viability was determined by CCK-8 assay.

Imaging of Lysosomes Rupture Induced by Inorganic Ions with Epo-LeuTyrAz/DBCORC and FITC-Sia. Epo-LeuTyr^{Az+}/^{DBCO}RC$^+$/FITC-Sia$^+$ HeLa cells were cultured for 48 h with no additions, SiO_2 (100 μg/mL), alums (150 μg/mL), CaO_x (100 μg/mL), or bismuth citrate (100 μM). The cells were washed with DMEM and then imaged with confocal microscopy.

RESULTS AND DISCUSSION

Labeling of Cathepsins in Lysosomes via BCCL. Epoxysuccinyl-leucine-tyrosine (Epo-LeuTyr) derivatives have been widely used to covalently modify the active site cysteine of cathepsins.[22,23,26] To fluorescently label cathepsins, we first prepared Epo-LeuTyr with C-terminal coumarin (Epo-LeuTyr-CM). Cells staining with Epo-LeuTyr-CM exhibited poor fluorescence in lysosomes, reflecting poor targeting of the substrate for lysosomes (Figure S1).

To overcome the incapability of preformed multifunctional probes to target cathepsins in lysosomes, we designed BCCL to optically tag cathepsins in live cells. As a proof of concept, we synthesized Epo-LeuTyr^{Az} with C-terminal azide (Scheme S1) and ^{DBCO}CM, a lysosome-specific dye containing a coumarin fluorophore linked to DBCO (^{DBCO}CM) (Figure 2).[27] ^{DBCO}CM could be enriched in lysosomes by acidotropic

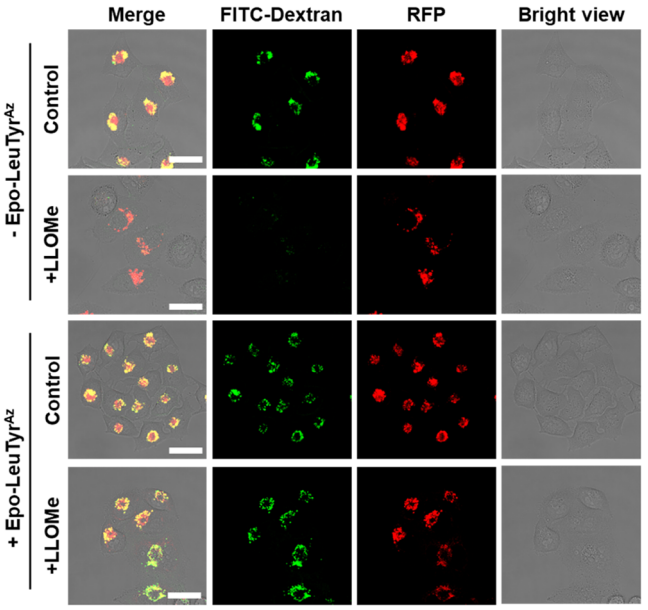

Figure 3. Effects of biocapture on catalysis of cathepsins. LAMP2-RFP$^+$ HeLa cells treated without or with Epo-LeuTyr^{Az} (20 μM,12 h) and then loaded with FITC-dextran (0.1 mg/mL, 12 h). The cells were further treated without or with LLOMe (3 mM) for 6 h and then imaged by confocal microscopy. Scale bars: 10 μm.

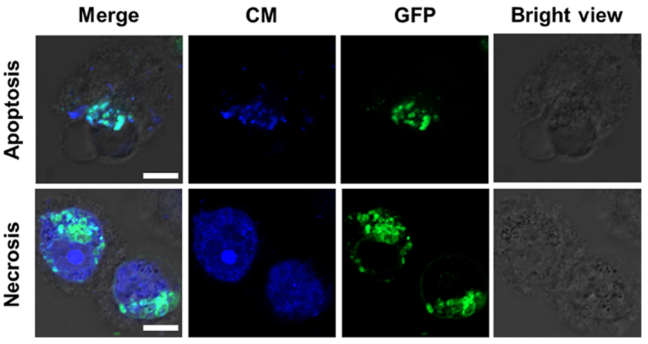

Figure 4. Imaging of lysosome rupture in necrosis by BCCL. LAMP2-GFP-RIP$_3^+$ HeLa cells prestained with Epo-LeuTyr^{Az}/^{DBCO}CM were treated for 5 h with TNF/Smac to induce apoptosis or with TNF/Smac/Z-VAD to trigger necrosis before confocal analysis. Scale bars: 10 μm.

effects due to protonation of the anime liner. In vitro reaction yields desired adduct from ^{DBCO}CM and Epo-LeuTyr^{Az}, as confirmed by mass spectrometry analysis (Figure S2), which is in line with the proposed SPAAC (Figure 2).

To achieve BCCL, HeLa cells expressing green fluorescent protein-fused lysosomal membrane-associated protein-2 (LAMP2-GFP) were cultured with Epo-LeuTyr^{Az} and then with ^{DBCO}CM, using cells stained with ^{DBCO}CM alone as the control. Both cell samples were further treated with no addition, Baf-A1, which is a potent inhibitor of ATPase and effectively neutralizes lysosomes,[28] or H_2O_2 to induce LMP.[15,29,30] We employed confocal microscopy to pinpoint ^{DBCO}CM compared to LAMP2-GFP, which is an integral constituent of lysosomes. We observed a loss of blue signals from lysosomes in control cells caused by Baf-A1 (Figure 2B), which is consistent with the dissipation of acidotropic dyes from neutralized lysosomes and LMP. To our delight, cells treated with Epo-LeuTyr^{Az} and ^{DBCO}CM maintained blue

https://doi.org/10.1021/acs.analchem.2c01892
Anal. Chem. 2022, 94, 9903−9910

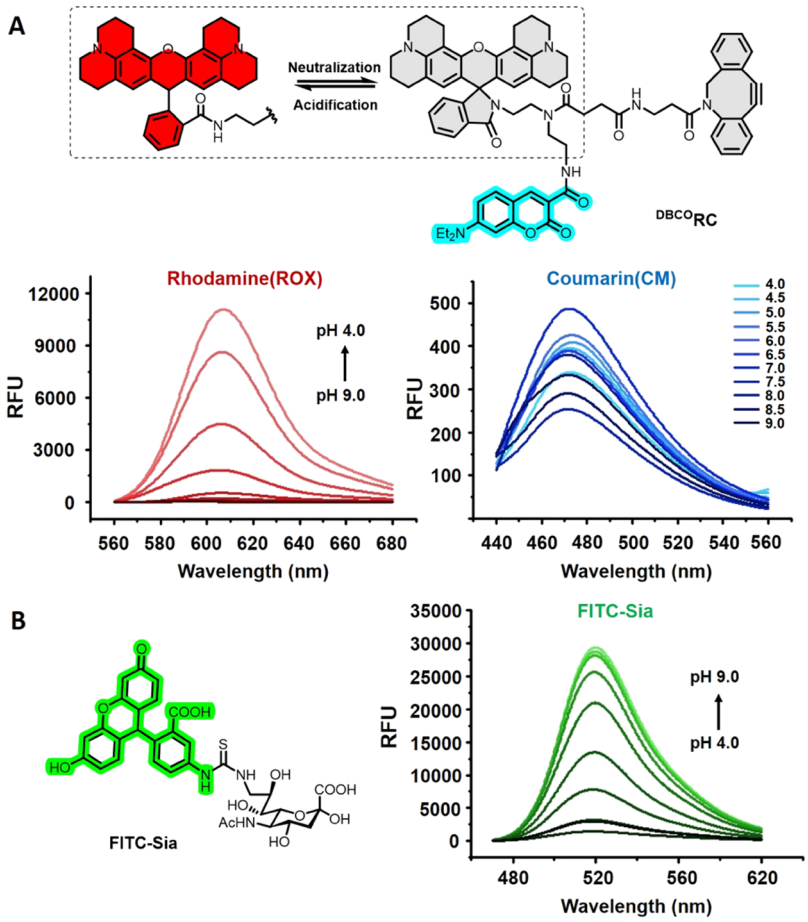

Figure 5. Chemical structure and pH responsiveness of ^{DBCO}RC and FITC-Sia. (A) Structure and pH responsiveness of ^{DBCO}RC undergoes acidity-triggered fluorogenic isomerization. (B) Structure and pH responsiveness of FITC-Sia.

fluorescence in lysosomes after treatment with Baf-A1. This showed that BCCL leads to signal retention in pH-elevated lysosomes. In addition, LAMP2-GFP$^+$/BCCL$^+$ cells exhibited retention of coumarin signals in lysosomes after treatment with H_2O_2 or methanol, another inducer of LMP (Figures 2C and S3). We then investigated the time and dose dependency of Epo-LeuTyr^{Az} and ^{DBCO}CM for BCCL in HeLa cells (Figures S4 and S5). The optimum condition was shown to be 20 μM and 12 h incubation for the former, while 10 μM and 2 h incubation for the latter. Together, these results showed retention of optically labeled cathepsin in LMP$^+$ lysosomes and pH-elevated lysosomes, confirming covalent labeling of cathepsin via BCCL.

As suicide substrates could inactivate cognate enzymes and because BCCL relies on the use of a suicide substrate, we thus examined the effect of BCCL on the catalytic activity of cathepsins. It was reported that LMP induced by L-leucyl-L-leucine-methyl ester (LLOMe) is dependent on the turnover of LLOMe by cysteine cathepsins.[16] Therefore, we assayed induction of LMP with LLOMe in LAMP2-RFP$^+$ HeLa cells treated with or without Epo-LeuTyr^{Az}. LLOMe results in loss of FITC-dextran from LAMP2-RFP$^+$ lysosomes in control cells free of Epo-LeuTyr^{Az}. However, Epo-LeuTyr^{Az+}/LLOMe$^+$ cells exhibited FITC-dextran stably trapped in lysosomes (Figure 3). This contrast showed inactivation of cathepsin by Epo-LeuTyr^{Az}, reflecting biocapture of Epo-LeuTyr^{Az} by the catalytically essential cysteine of cathepsins.

Imaging of Lysosome Rupture by BCCL. To make fluorescence stably trapped in pH-elevated and LMP$^+$ lysosomes, BCCL was further evaluated for its performance in lysosomal rupture. As lysosome rupture occurred in cell necrosis,[4] we applied Epo-LeuTyr^{Az}/^{DBCO}CM to LAMP2-GFP-RIP$_3^+$ HeLa cells. These cells were then treated with Smac/TNF/Z-VAD to induce necrosis or with Smac/TNF to induce apoptosis.[31] Confocal microscopic analysis revealed blue fluorescence stringently confined in lysosomes in cells undergoing apoptosis, whereas cells subjected to necrosis displayed blue fluorescence mostly located in cytosol (Figure 4). This reflects the release of fluorescently labeled cathepsins from lysosomes into cytosol during lysosomal rupture. Taken together, these results validate the capability of BCCL to discriminate ruptured lysosomes over pH-elevated and LMP$^+$ lysosomes.

Discern of Lysosomal Rupture over LMP via BCCL with a Ratiometric pH Sensor. After validating BCCL for imaging lysosome rupture over LMP, and because luminal pH is a key parameter of lysosomal status, we sought to label cathepsins with a lysosomal pH reporter. Hence, ^{DBCO}RC was synthesized to contain an amine-containing linker for acidotropic partition in acidic lysosomes, an entity of coumarin (CM) with "always-on" blue fluorescence, and an entity of ROX-lactam (ROX) with red fluorescence responsive to lysosomal acidity.[32] pH titration showed that ^{DBCO}RC displayed pH-inert blue fluorescence and acidity-triggered red fluorescence intensified as pH value decreased (Figure 5A),

https://doi.org/10.1021/acs.analchem.2c01892
Anal. Chem. 2022, 94, 9903−9910

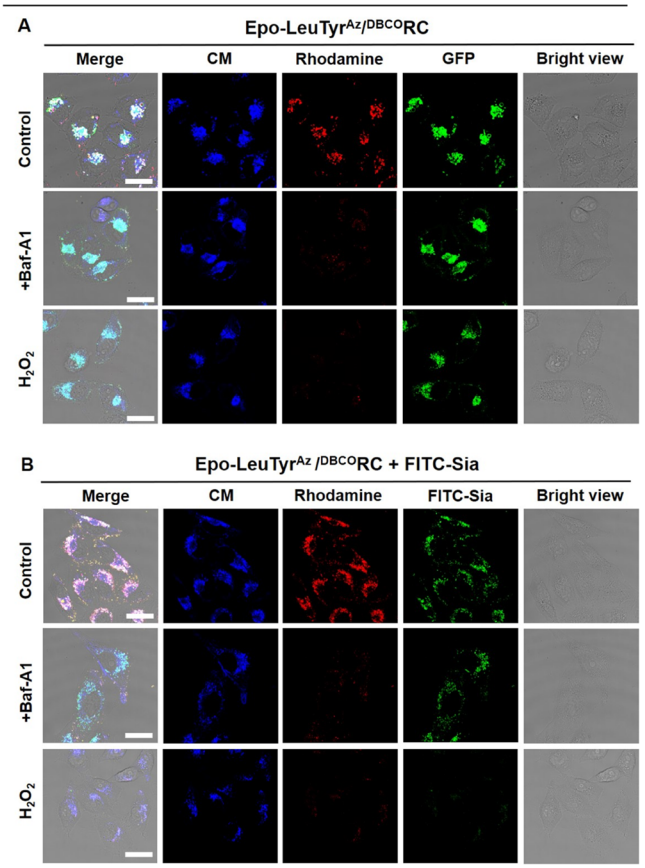

Figure 6. Discern of pH-elevated lysosomes over LMP$^+$ lysosomes by BCCL in combination with FITC-Sia. (A) Incapability of BCCL alone to discern pH-elevated lysosomes over LMP$^+$ lysosomes. ^{DBCO}RC$^+$/Epo-LeuTyr^{Az+} HeLa cells were cultured with Baf-A1 (100 nM) for 6 h or H_2O_2 (0.5 mM) for 1 h and then imaged by confocal microscopy. (B) Discern of pH-elevated lysosomes from LMP by BCCL/FITC-Sia. HeLa cells were cultured with Epo-LeuTyr^{Az} (20 μM) and FITC-Sia (10 μM) for 12 h, and then with ^{DBCO}RC (10 μM) for 2 h. The cells were further cultured with Baf-A1 (100 nM) for 6 h or H_2O_2 (0.5 mM) for 1 h prior to confocal microscopic analysis. Scale bars: 10 μm.

owing to proton-mediated fluorogenic isomerization of spirolactam.

We then applied ^{DBCO}RC to LAMP2-GFP$^+$ HeLa cells either alone or in combination with Epo-LeuTyr^{Az}. These cells were further stressed with Baf-A1. This caused complete loss of blue signals from lysosomes in ^{DBCO}RC$^+$ cells, showing failure of conventional acidotropic dyes to stain pH-elevated lysosomes (Figure S7). In contrast, ^{DBCO}RC$^+$/Epo-LeuTyr^{Az+} cells exhibited both red and blue fluorescence in lysosomes, showing the use of BCCL for dual-colored imaging of physiological lysosomes. Subsequent treatment with Baf-A1 caused the disappearance of red fluorescence, whereas the blue signal remained in lysosomes (Figure 6A). Similar imaging results were also obtained in HeLa cells subjected to H_2O_2-induced LMP. Retention of blue fluorescence is consistent with covalent labeling of ^{DBCO}RC to azide-modified cathepsins, while diminished red fluorescence showed the capability of BCCL aided with ^{DBCO}RC to discern pH-elevated lysosomes or LMP$^+$ lysosomes with blue signals over normal lysosomes exhibiting both red and blue fluorescence.

As BCCL could discriminate LMP from ruptured lysosomes but not pH-elevated lysosomes, and to discern different states of lysosomes, we explored the combination of BCCL with FITC-Sia (Figure 5B), a lysosomal probe that is trapped in pH-elevated lysosomes but readily dissipates from LMP[33] (Figure S6). Therefore, HeLa cells were subjected to BCCL with ^{DBCO}RC and then stained with FITC-Sia (Figure 6B). These cells were further stressed with Baf-A1 or H_2O_2. As expected, we observed blue and green fluorescence in pH-elevated lysosomes from cells treated with Baf-A1. In contrast, blue fluorescence was identified in LMP induced by H_2O_2, reflecting loss of FITC-Sia and lysosomal acidity upon LMP. Combined, these data showed the use of BCCL combined with FITC-Sia to distinguish pH-elevated lysosomes over LMP. Finally, our probes were shown to be of low cytotoxicity, which is beneficial for live cell imaging (Figure S8).

Effects of Inorganic Particles on Lysosomal Rupture. Inorganic materials that are frequently used to trigger lysosomal rupture include silicon dioxide (SiO_2)[34,35] and alums.[36,37] The former is employed as a delivery system, and the latter as vaccine adjuvants. In addition, bismuth has been utilized for the treatment of peptic ulcer.[38,39] Albeit widely used, the effects of these inorganic agents to trigger lysosome rupture have been largely undefined due to the lack of appropriate imaging methods. We were keen to apply BCCL/FITC-Sia to track lysosomes in HeLa cells treated with SiO_2, alums, bismuth citrate, as well as calcium oxalate (CaO_x)[5] highly related to oxalate nephropathy by inducing LMP.[40] Loss of red and green fluorescence was caused by SiO_2, alums, and CaO_x (Figure 7), showing dissipation of FITC-Sia from lysosomes and loss of lysosomal acidity. Differing from punctate blue fluorescence in CaO_x^+ cells, cells treated with SiO_2 or alum displayed scattered blue fluorescence throughout the cells, reflecting lysosomal rupture. These results showed that SiO_2 and alums are effective inducers of lysosomal rupture, whereas CaO_x triggers LMP. Accumulation of bismuth in lysosomes has been reported in kidney cells,[41] ganglion cells,[42] spinal cord motor neurons, and central neurons.[43,44] We observed blue, red, and green fluorescence in lysosomes from control cells and cells treated with bismuth citrate (Figure 7). Given the cell-type-dependent dramatic variation in the uptake of bismuth compounds,[45] we concluded that bismuth citrate is a minor stressor of lysosomes compared to SiO_2 and alums under our assay conditions. The results showed the utility of BCCL to assess the efficacy of lysosomal inducers that are increasingly employed for diverse biomedical purposes such as cancer treatment and vaccine development.

CONCLUSIONS

Lysosomal rupture is engaged in myriad diseases and also plays a role in drug release and immunomodulation. Current assays relying on acidotropic dyes or microbeads are often incapable of discerning ruptured lysosomes over pH-elevated lysosomes and LMP. We herein reported optical discern of lysosomal rupture with BCCL, based on tracking cathepsins in lysosomes or released into cytosol. BCCL-mediated cathepsin labeling is operated via covalent installation of an azide-tagged suicide substrate (Epo-LeuTyr^{Az}) to the enzyme active site, followed by bioorthogonal ligation of the introduced azide with ^{DBCO}RC, a ratiometric pH sensor featuring an acidity-reporting red fluorescence. Combined with FITC-Sia that is trapped in pH-elevated lysosomes but not LMP and ruptured lysosomes, BCCL enables optical discern of four states of lysosomes:

https://doi.org/10.1021/acs.analchem.2c01892
Anal. Chem. 2022, 94, 9903−9910

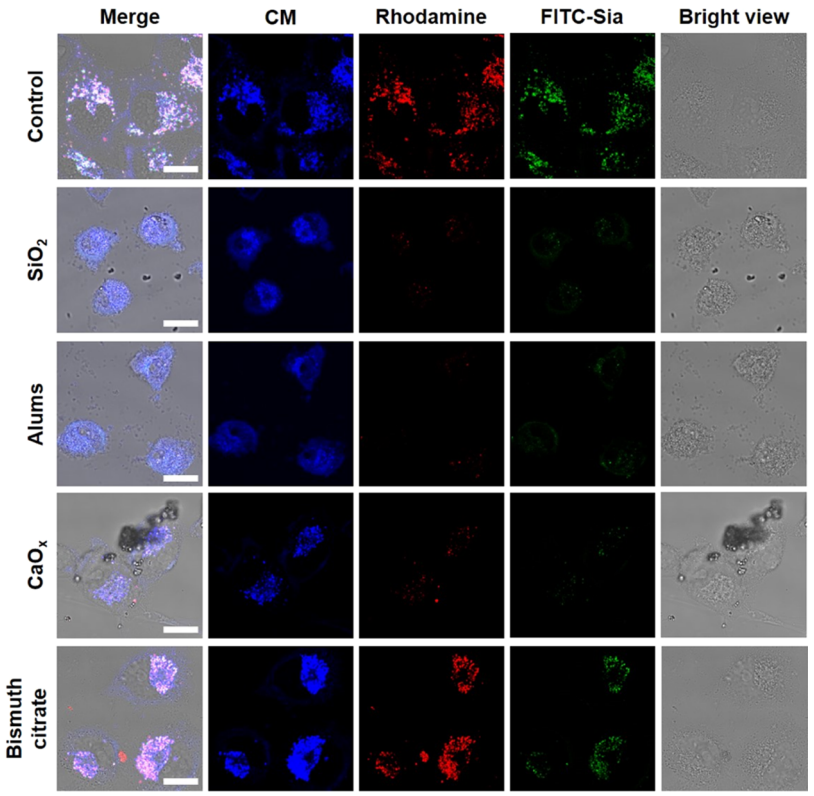

Figure 7. Lysosomal rupture caused by SiO_2 and alums. $BCCL^+$/FITC-Sia^+ HeLa cells were treated with SiO_2 (100 μg/mL), alums (150 μg/mL), CaO_x (100 μg/mL), bismuth citrate (100 μM), or no addition for 48 h prior to confocal microscopy analysis. Scale bars: 10 μm.

ruptured lysosomes (blue in cytosol), LMP^+ lysosomes (blue in lysosomes), pH-elevated lysosomes (blue and green in lysosomes), and physiological lysosomes (blue, green and red in lysosomes). This approach was further employed to investigate the effects of inorganic materials on lysosomes and revealed that SiO_2 and alums are effective lysosomal rupture inducers over CaO_x and bismuth. Our method holds the potential to study lysosome rupture over LMP in diseased cells and could be used to evaluate lysosome rupture-inducing agents.

■ ASSOCIATED CONTENT

Supporting Information

The Supporting Information is available free of charge at https://pubs.acs.org/doi/10.1021/acs.analchem.2c01892.

Content including synthesis and spectral analysis of new compounds, in vitro SPAAC of Epo-$LeuTyr^{Az}$ with ^{DBCO}CM, cell staining with Epo-LeuTyr-CM, dose- and time-dependent cell staining, probe selectivity and retention in pH-elevated lysosomes and LMP, and cytotoxicity of the probes (PDF)

■ AUTHOR INFORMATION

Corresponding Authors

Xinhui Su − *PET Center, Department of Nuclear Medicine, The First Affiliated Hospital, School of Medicine, Zhejiang University, Hangzhou 310003, China*; Phone: 86-0571-87236428; Email: suxinhui@zju.edu.cn

Shoufa Han − *Department of Chemical Biology, College of Chemistry and Chemical Engineering, State Key Laboratory for Physical Chemistry of Solid Surfaces, The Key Laboratory for Chemical Biology of Fujian Province, and The MOE Key Laboratory of Spectrochemical Analysis & Instrumentation, Xiamen University, Xiamen 361005, China*; orcid.org/0000-0002-2057-0559; Email: Shoufa@xmu.edu.cn

Authors

Lei Gao − *Department of Chemical Biology, College of Chemistry and Chemical Engineering, State Key Laboratory for Physical Chemistry of Solid Surfaces, The Key Laboratory for Chemical Biology of Fujian Province, and The MOE Key Laboratory of Spectrochemical Analysis & Instrumentation, Xiamen University, Xiamen 361005, China*

Yilong Shi − *College of Life Science and State Key Laboratory for Cell Stress, Xiamen University, Xiamen 361005, China*

Enkang Zhang − *Department of Chemical Biology, College of Chemistry and Chemical Engineering, State Key Laboratory for Physical Chemistry of Solid Surfaces, The Key Laboratory for Chemical Biology of Fujian Province, and The MOE Key Laboratory of Spectrochemical Analysis & Instrumentation, Xiamen University, Xiamen 361005, China*

Jinxuan You − *Department of Chemical Biology, College of Chemistry and Chemical Engineering, State Key Laboratory for Physical Chemistry of Solid Surfaces, The Key Laboratory for Chemical Biology of Fujian Province, and The MOE Key Laboratory of Spectrochemical Analysis & Instrumentation, Xiamen University, Xiamen 361005, China*

Jiahuai Han − *College of Life Science and State Key Laboratory for Cell Stress, Xiamen University, Xiamen 361005, China*

Complete contact information is available at: https://pubs.acs.org/10.1021/acs.analchem.2c01892

https://doi.org/10.1021/acs.analchem.2c01892
Anal. Chem. 2022, 94, 9903−9910

Author Contributions

The manuscript was written by L.G. and S.H.

Notes

The authors declare no competing financial interest.

■ ACKNOWLEDGMENTS

This work was supported by grants from NSFC (22177096 and 91854106). X.S. was supported by NSFC (82071965) and Huadong Medicine Joint Funds of the Zhejiang Provincial Natural Science Foundation of China (LHDMZ22H300010).

■ REFERENCES

(1) Zhu, S.-y.; Yao, R.; Li, Y.; Zhao, P.; Ren, C.; Du, X.; Yao, Y. *Cell Death Dis.* **2020**, *11*, 817.
(2) Ballabio, A.; Bonifacino, J. S. *Nat. Rev. Mol. Cell Biol.* **2020**, *21*, 101−118.
(3) Aits, S.; Jäättelä, M. *J. Cell Sci.* **2013**, *126*, 1905−1912.
(4) Lima, H., Jr.; Jacobson, L.; Goldberg, M.; Chandran, K.; Diaz-Griffero, F.; Lisanti, M. P.; Brojatsch, J. *Cell Cycle* **2013**, *12*, 1868−1878.
(5) Nakamura, S.; Shigeyama, S.; Minami, S.; Shima, T.; Akayama, S.; Matsuda, T.; Esposito, A.; Napolitano, G.; Kuma, A.; Namba-Hamano, T.; Nakamura, J.; Yamamoto, K.; Sasai, M.; Tokumura, A.; Miyamoto, M.; Oe, Y.; Fujita, T.; Terawaki, S.; Takahashi, A.; Hamasaki, M.; Yamamoto, M.; Okada, Y.; Komatsu, M.; Nagai, T.; Takabatake, Y.; Xu, H.; Isaka, Y.; Ballabio, A.; Yoshimori, T. *Nat. Cell Biol.* **2020**, *22*, 1252−1263.
(6) Gao, C.; Ding, Y.; Zhong, L.; Jiang, L.; Geng, C.; Yao, X.; Cao, J. *Toxicol. In Vitro* **2014**, *28*, 667−674.
(7) Gao, C.; Zhong, L.; Jiang, L.; Geng, C.; Yao, X.; Cao, J. *Phytomedicine* **2013**, *20*, 705−709.
(8) Burgener, S. S.; Leborgne, N. G. F.; Snipas, S. J.; Salvesen, G. S.; Bird, P. I.; Benarafa, C. *Cell Rep.* **2019**, *27*, 3646−3656.e5.
(9) Xu, M.; Yang, L.; Rong, J.-G.; Ni, Y.; Gu, W.-W.; Luo, Y.; Ishidoh, K.; Katunuma, N.; Li, Z.-S.; Zhang, H.-L. *Glia* **2014**, *62*, 855−880.
(10) Zou, J.; Kawai, T.; Tsuchida, T.; Kozaki, T.; Tanaka, H.; Shin, K.-S.; Kumar, H.; Akira, S. *Immunity* **2013**, *38*, 717−728.
(11) Keum, C.; Hong, J.; Kim, D.; Lee, S.-Y.; Kim, H. *ACS Appl. Mater. Interfaces* **2021**, *13*, 14866−14874.
(12) Nandi, D.; Shivrayan, M.; Gao, J.; Krishna, J.; Das, R.; Liu, B.; Thayumanavan, S.; Kulkarni, A. *ACS Appl. Mater. Interfaces* **2021**, *13*, 45300−45314.
(13) Baljon, J. J.; Dandy, A.; Wang-Bishop, L.; Wehbe, M.; Jacobson, M. E.; Wilson, J. T. *Biomater. Sci.* **2019**, *7*, 1888−1897.
(14) Maejima, I.; Takahashi, A.; Omori, H.; Kimura, T.; Takabatake, Y.; Saitoh, T.; Yamamoto, A.; Hamasaki, M.; Noda, T.; Isaka, Y.; Yoshimori, T. *EMBO J.* **2013**, *32*, 2336−2347.
(15) Gao, L.; Han, S. *Anal. Chem.* **2021**, *93*, 12639−12647.
(16) Repnik, U.; Distefano, M. B.; Speth, M. T.; Ng, M. Y. W.; Progida, C.; Hoflack, B.; Gruenberg, J.; Griffiths, G. *J. Cell Sci.* **2017**, *130*, 3124−3140.
(17) Verdoes, M.; Oresic Bender, K.; Segal, E.; van der Linden, W. A.; Syed, S.; Withana, N. P.; Sanman, L. E.; Bogyo, M. *J. Am. Chem. Soc.* **2013**, *135*, 14726−14730.
(18) Blum, G.; von Degenfeld, G.; Merchant, M. J.; Blau, H. M.; Bogyo, M. *Nat. Chem. Biol.* **2007**, *3*, 668−677.
(19) Segal, E.; Prestwood, T. R.; van der Linden, W. A.; Carmi, Y.; Bhattacharya, N.; Withana, N.; Verdoes, M.; Habtezion, A.; Engleman, E. G.; Bogyo, M. *Chem. Biol.* **2015**, *22*, 148−158.
(20) Hillaert, U.; Verdoes, M.; Florea, B. I.; Saragliadis, A.; Habets, K. L. L.; Kuiper, J.; VanCalenbergh, S.; Ossendorp, F.; vanderMarel, G. A.; Driessen, C.; Overkleeft, H. S. *Angew. Chem., Int. Ed.* **2009**, *48*, 1629−1632.
(21) Fan, F.; Nie, S.; Yang, D.; Luo, M.; Shi, H.; Zhang, Y.-H. *Bioconjugate Chem.* **2012**, *23*, 1309−1317.
(22) Pan, D.; Hu, Z.; Qiu, F.; Huang, Z.-L.; Ma, Y.; Wang, Y.; Qin, L.; Zhang, Z.; Zeng, S.; Zhang, Y.-H. *Nat. Commun.* **2014**, *5*, No. 5573.
(23) Han, Y.; Li, M.; Qiu, F.; Zhang, M.; Zhang, Y.-H. *Nat. Commun.* **2017**, *8*, No. 1307.
(24) Zhang, E.; Shi, Y.; Han, J.; Han, S. *Anal. Chem.* **2020**, *92*, 15059−15068.
(25) Shi, Y.; Zou, X.; Wen, S.; Gao, L.; Li, J.; Han, J.; Han, S. *Autophagy* **2021**, *17*, 3475−3490.
(26) Ji, C.; Liang, Y.; Ge, F.; Yang, L.; Wang, Q. *Anal. Chem.* **2019**, *91*, 7032−7038.
(27) Zhang, E.; Shi, Y.; Han, J.; Han, S. *Anal. Chem.* **2020**, *92*, 15059−15068.
(28) Furuchi, T.; Aikawa, K.; Arai, H.; Inoue, K. *J. Biol. Chem.* **1993**, *268*, 27345−27348.
(29) Lin, L.-S.; Huang, T.; Song, J.; Ou, X.-Y.; Wang, Z.; Deng, H.; Tian, R.; Liu, Y.; Wang, J.-F.; Liu, Y.; Yu, G.; Zhou, Z.; Wang, S.; Niu, G.; Yang, H.-H.; Chen, X. *J. Am. Chem. Soc.* **2019**, *141*, 9937−9945.
(30) Gao, W.; Cao, W.; Zhang, H.; Li, P.; Xu, K.; Tang, B. *Chem. Commun.* **2014**, *50*, 8117−8120.
(31) He, S.; Wang, L.; Miao, L.; Wang, T.; Du, F.; Zhao, L.; Wang, X. *Cell* **2009**, *137*, 1100−1111.
(32) Xue, Z.; Zhang, E.; Liu, J.; Han, J.; Han, S. *Angew. Chem., Int. Ed.* **2018**, *57*, 10096−10101.
(33) Wu, X.; Tian, Y.; Yu, M.; Lin, B.; Han, J.; Han, S. *Biomater. Sci.* **2014**, *2*, 1120−1127.
(34) Hornung, V.; Bauernfeind, F.; Halle, A.; Samstad, E. O.; Kono, H.; Rock, K. L.; Fitzgerald, K. A.; Latz, E. *Nat. Immunol.* **2008**, *9*, 847−856.
(35) Roy, I.; Ohulchanskyy, T. Y.; Bharali, D. J.; Pudavar, H. E.; Mistretta, R. A.; Kaur, N.; Prasad, P. N. *Proc. Natl. Acad. Sci. U.S.A.* **2005**, *102*, 279−284.
(36) Sharp, F. A.; Ruane, D.; Claass, B.; Creagh, E.; Harris, J.; Malyala, P.; Singh, M.; O'Hagan, D. T.; Pétrilli, V.; Tschopp, J.; O'Neill, L. A. J.; Lavelle, E. C. *Proc. Natl. Acad. Sci. U.S.A.* **2009**, *106*, 870−875.
(37) Hem, S. L.; HogenEsch, H. *Expert Rev. Vaccines* **2007**, *6*, 685−698.
(38) Stoltenberg, M.; Larsen, A.; Zhao, M.; Danscher, G.; Brunk, U. T. *Apmis* **2002**, *110*, 396−402.
(39) Griffith, D. M.; Li, H.; Werrett, M. V.; Andrews, P. C.; Sun, H. *Chem. Soc. Rev.* **2021**, *50*, 12037−12069.
(40) Waikar, S. S.; Srivastava, A.; Palsson, R.; Shafi, T.; Hsu, C.; Sharma, K.; Lash, J. P.; Chen, J.; He, J.; Lieske, J.; Xie, D.; Zhang, X.; Feldman, H. I.; Curhan, G. C. *JAMA Intern. Med.* **2019**, *179*, 542−551.
(41) Stoltenberg, M.; Danscher, G. *Histochem. J.* **2000**, *32*, 645−652.
(42) Stoltenberg, M.; Schiønning, J. D.; Danscher, G. *Acta Neuropathol.* **2001**, *101*, 123−128.
(43) Pamphlett, R.; Stoltenberg, M.; Rungby, J.; Danscher, G. *Neurotoxicol. Teratol.* **2000**, *22*, 559−563.
(44) Pamphlett, R.; Danscher, G.; Rungby, J.; Stoltenberg, M. *Environ. Res.* **2000**, *82*, 258−262.
(45) von Recklinghausen, U.; Hartmann, L. M.; Rabieh, S.; Hippler, J.; Hirner, A. V.; Rettenmeier, A. W.; Dopp, E. *Chem. Res. Toxicol.* **2008**, *21*, 1219−1228.

https://doi.org/10.1021/acs.analchem.2c01892
Anal. Chem. 2022, 94, 9903−9910